Steel and Composite Structures, *Vol. 19, No. 6 (2015) 1549-1560*
DOI: http://dx.doi.org/10.12989/scs.2015.19.6.1549

Fatigue crack effect on magnetic flux leakage for A283 grade C steel

M.I.M. Ahmad*, A. Arifin [a], S. Abdullah [b], W.Z.W. Jusoh and S.S.K. Singh

Department of Mechanical & Materials Engineering, Faculty of Engineering and Build Environments, Universiti Kebangsaan Malaysia, 43600 UKM Bangi, Selangor, Malaysia

(*Received November 19, 2014, Revised July 08, 2015, Accepted July 11, 2015*)

Abstract. This paper presents the characterization of fatigue crack in the A283 Grade C steel using the MMM method by identifying the effects of magnetic flux leakage towards the crack growth rate, *da/dN*, and crack length.The previous and current research on the relation between MMM parameters and fatigue crack effect is still unclear and requires specific analysis to validate that. This method is considered to be a passive magnetic method among other Non-Destructive Testing (NDT) methods. The tension-tension fatigue test was conducted with a testing frequency of 10 Hz with 4 kN loaded, meanwhile the MMM response signals were captured using a MMM instrument. A correlation between the crack growth rate and magnetic flux leakage produces a sigmoid shape curve with a constant values which present the gradient, m value is in the ranges of 1.4357 to 4.0506, and the y-intercept, log C in the ranges of 4×10^{-7} to 0.0303. Moreover, a linear relation was obtained between the crack length and magnetic flux leakage which present the R-Squared values is at 0.830 to 0.978. Therefore, MMM method has their own capability to investigate and characterize the fatigue crack effects as a main source of fracture mechanism for ferrous-based materials.

Keywords: fatigue crack effect; MMM signal response; magnetic flux leakage; crack growth rate; crack length

1. Introduction

Recently, the majority of engineering industrial fields, such as aerospace, automotive, railway, or pipeline, have been concerned with the fatigue fracture of metals that have the ability to be subjected to variable loadings in service (Xing *et al*. 2006, Dong *et al*. 2010a, b, Zhang *et al*. 2012). For instance, failure in large storage tanks which have been built using A283 Grade C steel have occurred from time to time and the results were involved many destructions and losses of property and money (Milne *et al*. 2003).

On certain occasions, structural failure often occurs as a result of fatigue (Dubov 1997). Hence, evaluating fatigue damage and predicting the remaining fatigue life, plays an important role in preventing the metals from failure. The fatigue cracks that occur on ferromagnetic material

∗Corresponding author, E-mail: meoriqram@ukm.edu.my
[a] E-mail: azli@eng.ukm.my
[b] E-mail: shahrum@eng.ukm.my

http://www.techno-press.org/?journal=scs&subpage=8 ISSN: 1229-9367 (Print), 1598-6233 (Online)

surfaces are initiated and induced spontaneously through a fluctuation of magnetic signals. This propagates to a critical crack size that has stress concentration zones or micro-defects until the structure fails. Stress Concentration Zones (SCZ) are the main factors that affect the development of fatigue fractures (Xing *et al*. 2006, Zhang *et al*. 2012). By taking these SCZ as a variable, the MMM method can be used to detect SCZ by referring to the Self-Magnetic Leakage Field (SMLF) distribution on metal surfaces.

Apart from SCZ, the MMM method can also detect macroscopic cracks and defects at an early stage. In fact, the MMM method also has the potential for fatigue damage evaluation and remaining life prediction (Dubov 1997, Dong *et al*. 2010a, b, Xing *et al*. 2007, Yang *et al*. 2013, Wu *et al*. 2010). There are many previous and ongoing researches in this field. In a previous review, Xing *et al*. (2006) discussed the MMM method for fatigue damage evaluation and remaining life prediction in a rotary bending fatigue test. This was followed by Dong *et al*. (2008) who discussed monitoring fatigue damage, detecting the initiation and propagation of fatigue cracks, and predicting residual stress using spontaneous abnormal magnetic signals. Furthermore, Dong *et al*. (2010a) discussed MMM signal characteristics in the tension-tension fatigue testing of notched plate specimens; and reported that the MMM signals are intensively affected by many factors, such as different load types, machining processes, heat treatment conditions, and extra magnetic fields, which prevent MMM testing from being widely used in practical projects. This was further enhanced by Xing *et al*. (2007) in studying the correlation between the crack growth rate, da/dN, and magnetic memory signal $Hp(y)$ through a three-point bending fatigue testing. Wang *et al*. (2012) also reviewed the fundamentals of MMM technology as an effective method in assessing the early damage and defects by detecting the surface of metal depth of up to several millimeters with a maximum measuring velocity of up to several meters per second.

However, little research has focused on this method, such as the deficiency of physical criteria of relations between MMM signals with tensile fatigue damage and the accuracy of MMM signals during detecting the position of the crack damage in a metal. Although many previous researchers used this method, it is still necessary to conduct further research to attain a better understanding of this method and to find a better correlation for the MMM method and fatigue analysis. In this study, through tensile fatigue experiments, the authors investigated the characterization of fatigue crack for A283 Grade C steel, using a MMM technique, by referring to a study on the effect of magnetic flux leakage on metal components. This paper is more focused on finding the correlation of the crack growth rate and the crack length with MMM signals due to fatigue, and its significance in detecting the failure of materials.

2. Theoretical background of metal magnetic memory

The application of MMM gives an opportunity to perform a 100% equipment examination with detecting of SCZ and defects at an early stage of their development (Dubov *et al*. 2006). MMM inspection uses natural magnetization and the after-effect, which appears in the form of the magnetic memory of the metal to actual strains and structural changes of metal and no preparatory operation are required. For example of case, a rectangular defect zone of the specimen with 2b (mm) in width and h (mm) in depth (as shown in Fig. 1). When a defect presents, stress releases quickly and demagnetization increases rapidly, therefore opposite magnetic charges are accumulated on either side of the notch. As a result, two magnetic charge planes are formed with same magnetic charge density, ρ_m and opposite magnetic pole. Therefore, the magnetic flux

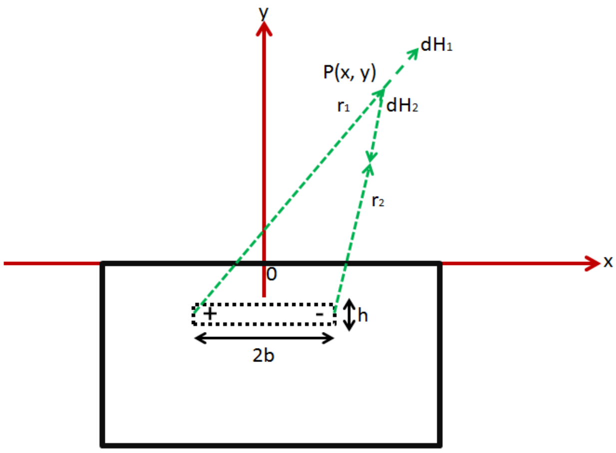

Fig. 1 Magnetic flux leakage field at a space point, $P(x, y)$ based on Equivalent Plane Dipole model

leakage field at the space point, $P(x, y)$ can be expressed as

$$\begin{aligned} dH_1 &= \frac{\rho_m \, . \, d\eta}{2\pi\mu_0 r_1^2} r_1 \\ dH_2 &= \frac{\rho_m \, . d\eta}{2\pi\mu_0 r_2^2} r_2 \end{aligned} \tag{1}$$

where $r_1 = \sqrt{(x+b)^2 + (y+\eta)^2}$, $r_2 = \sqrt{(x-b)^2 + (y+\eta)^2}$, dη is the width of magnetic charges and μ_0 is the permeability in vacuum. Then, the normal component of magnetic flux leakage field, $H_p(y)$ at $P(x, y)$ can be performed in Eq. (2) (Huang *et al*. 2014).

$$\begin{aligned} Hp(y) &= \int_{-h}^{0} dH_{1y} + \int_{-h}^{0} dH_{2y} \\ &= \int_{-h}^{0} \frac{\rho_m (y + \eta) d\eta}{2\pi\mu_0 \, [(x+b)^2 + (y+\eta)^2]} + \int_{-h}^{0} \frac{(-\rho_m)(y+\eta) d\eta}{2\pi\mu_0 [(x-b)^2 + (y+\eta)^2]} \\ &= \frac{\rho_m}{4\pi\mu_0} \left[ln \frac{(x+b)^2 + (y+h)^2}{(x+b)^2 + y^2} - ln \frac{(x-b)^2 + (y+h)^2}{(x-b)^2 + y^2} \right] \end{aligned} \tag{2}$$

The fatigue crack growth prediction model is a fracture mechanics based models that have been developed to support the damage tolerance concepts in metallic structures. This is categorized according to the type of loading and the concept of model is described. The first paper was published by Paris *et al*. that introduced the correlation between the crack growth rate, da/dN and the stress intensity factor range, ΔK (Beden *et al*. 2009). The results of the crack growth tests were expressed a linear relation between log (da/dN) and log (ΔK) which led to the well-known Paris equation as shown in Eq. (3)

$$\frac{da}{dN} = C(\Delta K) \tag{3}$$

with C and m as experimentally obtained constants. The equation is a formal description of the results of a fatigue crack growth experiment. From here, the Eq. (3) can be manipulated to find the correlation factor between the magnetic flux leakage, $Hp(y)$ with the crack growth rate, da/dN by replacing the position of ΔK with $Hp(y)$ and this can be seen in Equations below

$$\frac{da}{dN} = C[Hp(y)]m \tag{4}$$

$$\log\left(\frac{da}{dN}\right) = log\ C + m[log\ Hp(y)] \tag{5}$$

which log C is a y-intercept and m is a gradient of the graph between log $(\frac{da}{dN})$ and log $H_p(y)$.

3. Materials and methods

3.1 Specimen preparation

The specimens were fabricated from an A283 Grade C steel plate, which was chosen as the testing material due to its common use in heavy engineering applications, such as the manufacture

Table 1 Chemical composition (*wt %*) of A283 Grade

Carbon, C	Copper, Cu	Iron, Fe	Manganese, Mn	Phosphorus, P	Silicon, Si	Sulpfur, S
0.24	≥ 0.20	98.00	0.90	0.04	0.04	0.05

Table 2 Mechanical properties of A283 Grade C steel

Ultimate tensile strength, MPa	Yield strength, MPa	Elongation, %	Bulk modulus, MPa	Shear modulus, GPa
380 - 485	205	25	140	80

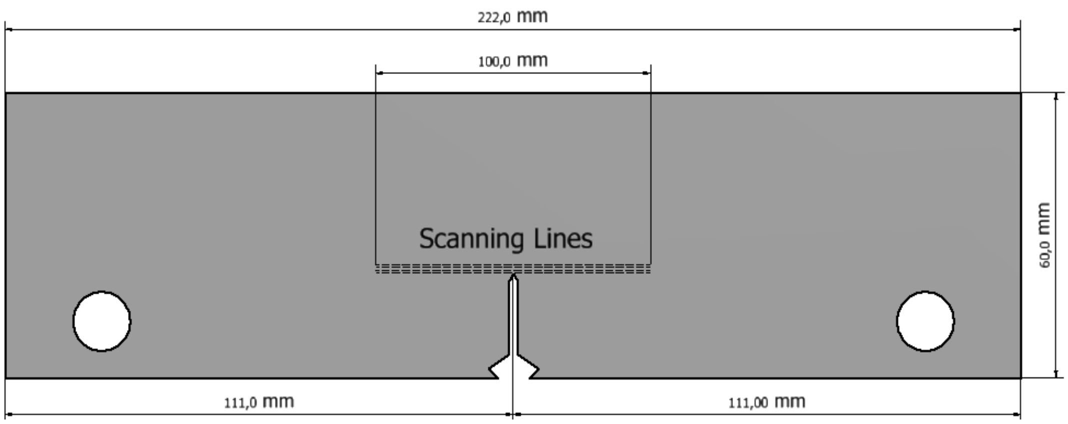

Fig. 2 Geometry dimensions of the notched fatigue specimen and the scanning line of the MMM signals

of storage tanks, vessels, and structural applications. The high possibility of this material being exposed to failure during operations was taken into consideration in order to develop this case work. The chemical composition and mechanical properties of A283 Grade C steel are shown in Tables 1-2 (C33, Standard Specification for Concrete Aggregrates). Detailed information about this material is extremely important, in order to familiarize ourselves with its strength capabilities before starting the experiment.

Specimens with 3 mm thicknesses were used for this experiment, designed according to ASTM: E647, International and Material (as shown in Fig. 2). A scanning line, with a length of 100 mm, was made to be vertical to the crack starter notch's centre.

3.2 Experimental procedure

The fatigue test was conducted using an INSTRON 8801, 100 kN, servo-hydraulic machine (as shown in Fig. 3). In order to observe the stable crack growth propagation, a tension-tension fatigue test, with a testing frequency of 10 Hz and a loading stress of 150 MPa, was applied during the test.

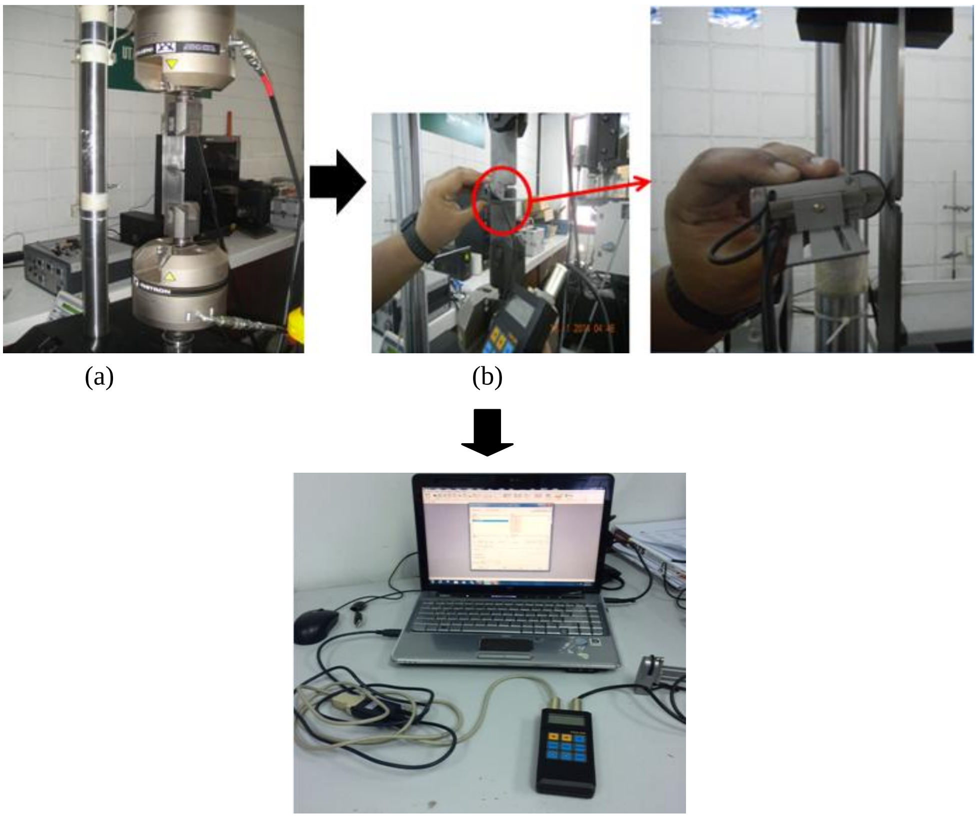

(a) (b) (c)

Fig. 3 Fatigue test set-up. (a) The servo-hydraulic machine with a specimen attached; (b) scanning process using MMM instrument; (c) MMM data collection through the computer using TSC-MMM-3.0 Software

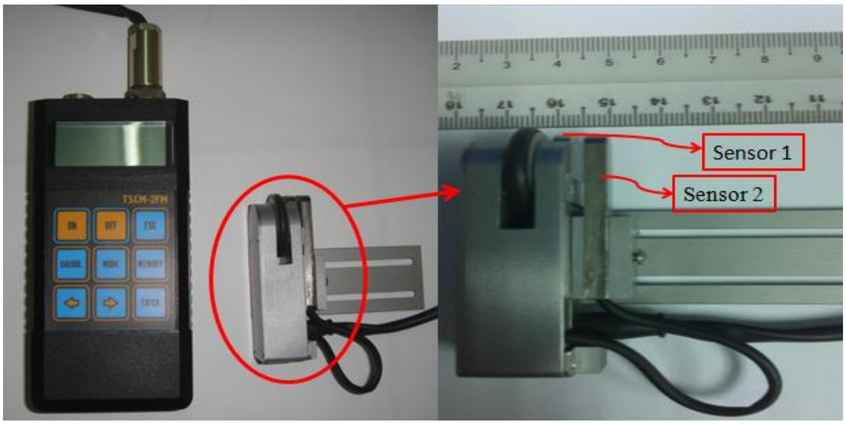

Fig. 4 The MMM instrument and scanning device

Fig. 5 A EUROMAX PB4161 microscope

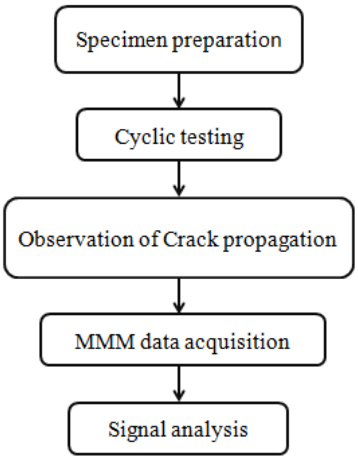

Fig. 6 Process flow of experimental method

A microscope (as shown in Fig. 5) was used to observe the beginning of crack propagation on the specimen's surface.

A scanning line, with a length of 100 mm, was made to be vertical to the crack starter notch's centre, so that the recorded data taken would be passed through the SCZ and the normal zone. Moreover, the line was placed 2 mm from the crack starter notch, in order to prevent the MMM sensors from detecting the notch area only. The specimen was scanned using the MMM instrument during the experiment, in order to measure the MMM signals by continuously scanning. At the same time, this instrument displayed the measured data of the magnetic leakage field, Hp versus scanning distance. The fatigue test was paused at predetermined cycles during the MMM scanning of the specimen's surface. This entire procedure was repeated for another two specimens using the same loads and dimensions, in order to increase the variety and comparability of the obtained data. The process flow of the experimental method is shown in Fig. 6.

4. Results and discussion

4.1 The formation of magnetic signals

The Figures above show the intensity of magnetic flux signal which is based on the extension of crack length (1 mm to 8 mm) for all specimens. From here, a big changed (abnormal magnetic peak) was observed at a distance of 45 mm to 55 mm toward the magnetic flux signal on the surface of the specimen. The drastic changed is caused by the high values of stress, σ_o that produced due to the increasing of fatigue load cycles where the notched of the specimen was placed in this area. The extreme stress that formed will enhance the formation of SCZs and the possibility in this area's to fail is very high. From the results obtained, it was found that the detection of cracked position can be determined easily and this gives the advantage to the MMM method as a one medium to detect the position of the crack in the metal before it fails.

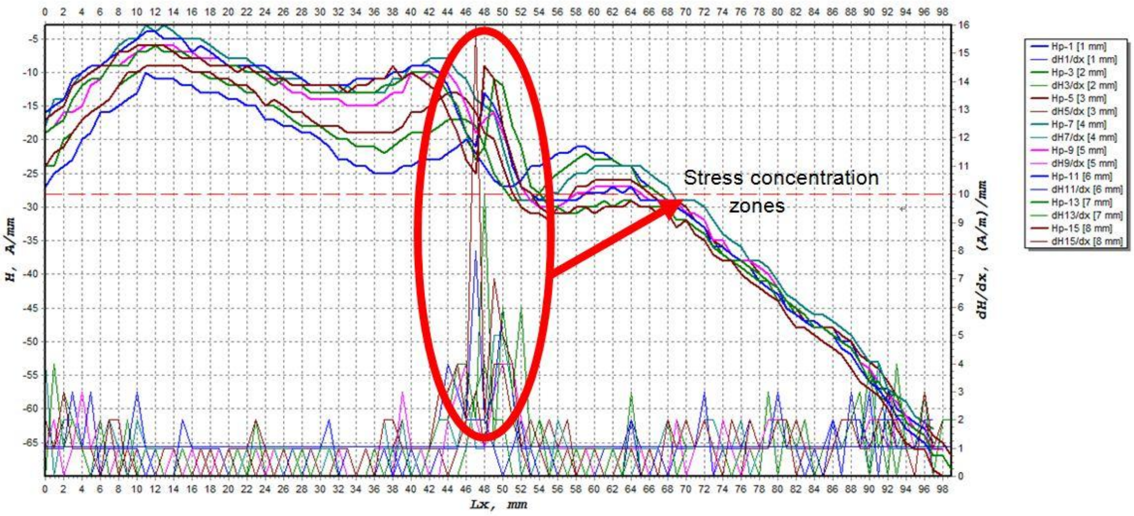

Fig. 7 The amplitude of SMLF signals, $Hp(y)$ and dH/dx for specimen 1

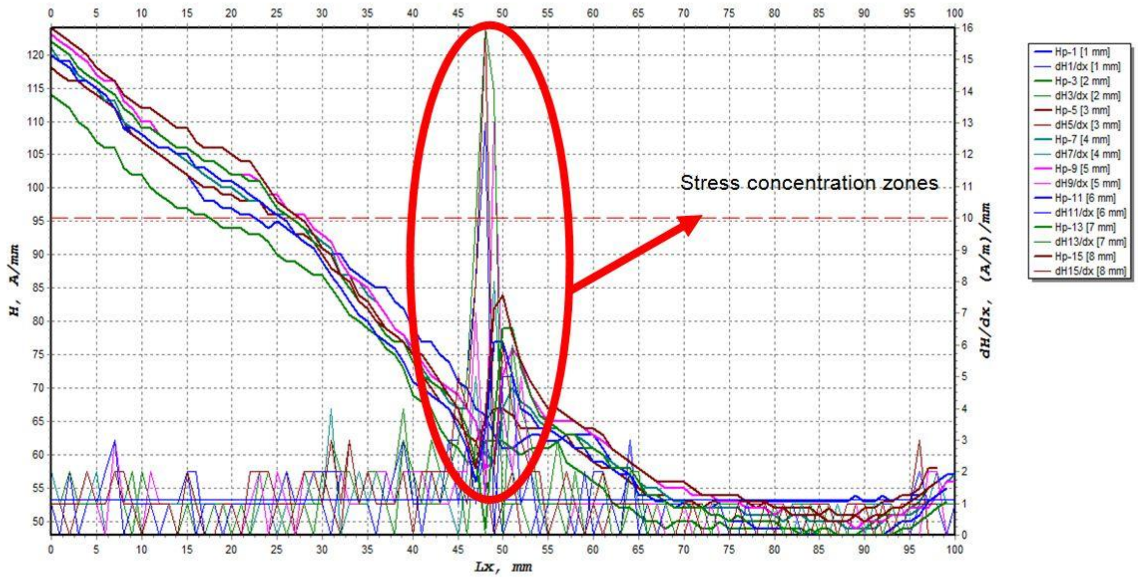

Fig. 8 The amplitude of SMLF signals, *Hp*(*y*) and *dH*/*dx* for specimen 2

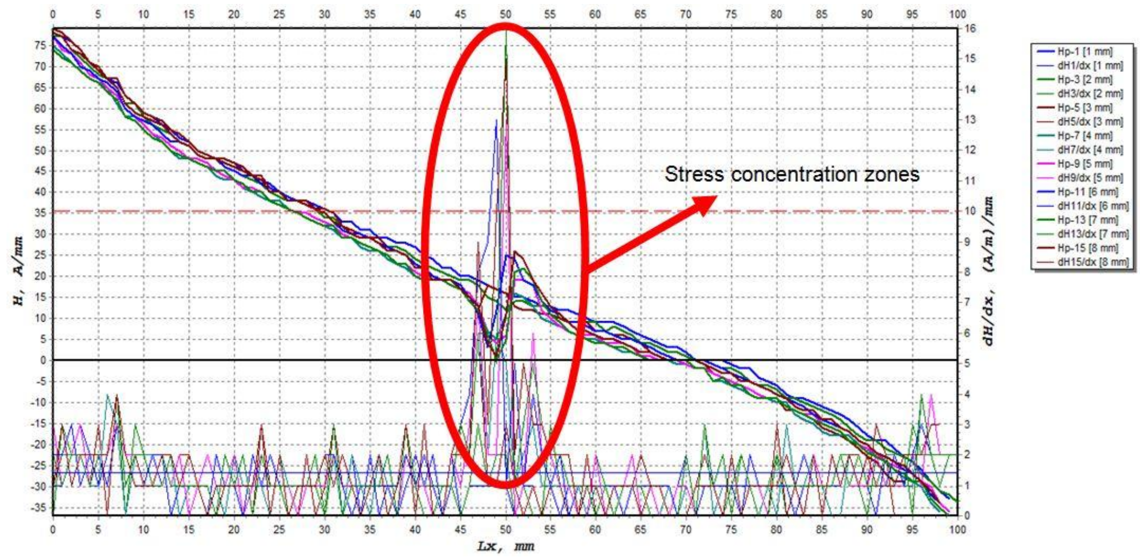

Fig. 9 The amplitude of SMLF signals, *Hp*(*y*) and *dH*/*dx* for specimen 3

4.2 The crack growth rate and magnetic flux leakage relation

Fig. 10 shows the propagation of crack growth on metal surfaces during the fatigue test. This occurred because of the slippage in the crystalline structure, which led to the formation of a micro-crack on the specimen. When the micro-cracks begin to form, the formation of macro-cracks will take place and cause a failure of the specimen.

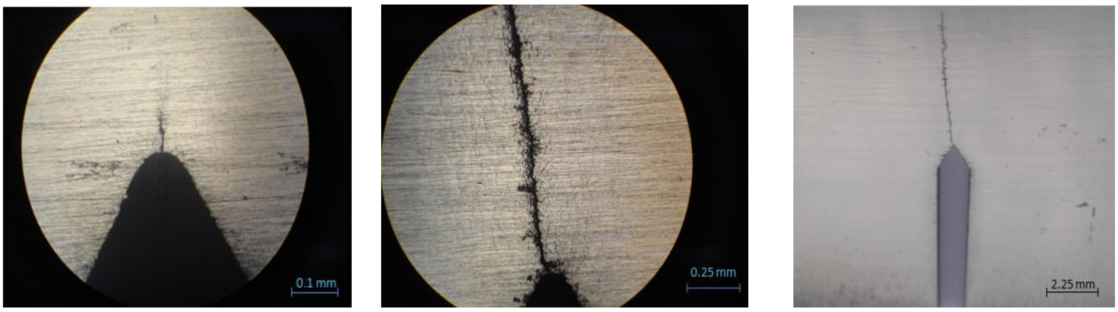

(a) (b) (c)

Fig. 10 Microscopic images of the crack at the initial notch at certain cycles. These images are magnified to 25x, 10x, and 1x sizes

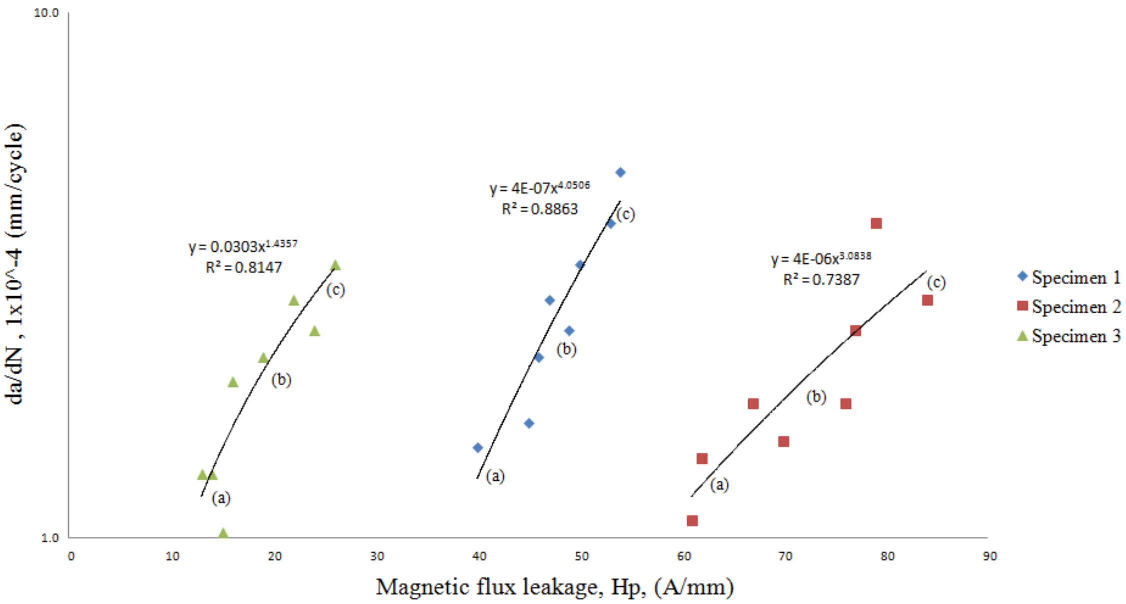

Fig. 11 Correlation between crack growth rate and magnetic flux leakage from the MMM signals

Furthermore, Fig. 11 shows the relationship between *da*/*dN* and *Hp*(*y*) for A283 Grade C steel during the tension-tension fatigue test. In graphical observation, the rate of crack growth, *da*/*dN*, was increased simultaneously with the increasing of magnetic flux leakage towards the surface of the metal with the R-Squared values in the range of 0.7387 to 0.8863 respectively. It can also be clearly seen that the patterns of the curves (for all specimens) showed an identical trend, with a sigmoid shape (Xing *et al*. 2007).

From here, three regions of behaviour are indicated. At an early stage, a crack starts to grow near to the region (a) (also known as crack nucleation). Theoretically, the changes of *Hp*(*y*) will affect the value of stress intensity range, ΔK_{th}. After the crack growth propagates beyond the region (b), the *da*/*dN* and *Hp*(*y*) relationship follows a power equation (as shown in Eq. (4)) that yields a straight line on the logarithmic coordinates. Moreover, under the region (*c*), the high value of *Hp*(*y*) promotes an unstable rapid crack growth rate, which enhances rapidly to fracture. Due to increasing of the fatigue load cycles, it will accumulate a dislocation that influences the crack propagation. As a result, it grows into a micro-crack that eventually propagates to a macro-crack until the specimen fails. The early stages of the crack growth usually occur when load cycles are applied to a first cycle of up to 10% of the total cycles to fracture (Dong *et al*. 2010a, b, Xing *et al*. 2007, Dowling 1993).

From here, three regions of behaviour are indicated. At an early stage, a crack starts to grow near to the region (a) (also known as crack nucleation). Theoretically, the changes of *Hp*(*y*) will affect the value of stress intensity range, ΔK_{th}. After the crack growth propagates beyond the region (b), the *da*/*dN* and *Hp*(*y*) relationship follows a power equation (as shown in Eq. (4)) that yields a straight line on the logarithmic coordinates. Moreover, under the region (*c*), the high value of *Hp*(*y*) promotes an unstable rapid crack growth rate, which enhances rapidly to fracture. Due to increasing of the fatigue load cycles, it will accumulate a dislocation that influences the crack propagation. As a result, it grows into a micro-crack that eventually propagates to a macro-crack until the specimen fails. The early stages of the crack growth usually occur when load cycles are applied to a first cycle of up to 10% of the total cycles to fracture (Dong *et al*. 2010, Xing *et al*. 2007, Dowling 1993).

4.3 The crack length and magnetic flux leakage field, Hp relation

For further analysis, the relationship between the crack length and magnetic flux leakage field was investigated (as shown in Fig. 12).

Fig. 12 shows that when the magnetic flux leakage increased during the experiment, the length of the crack also increased with the ranges of R-Squared value is at 0.830 to 0.978. This hypothesis is made because during a crack extension, the crack cuts-off the path of the Earth's magnetic lines,

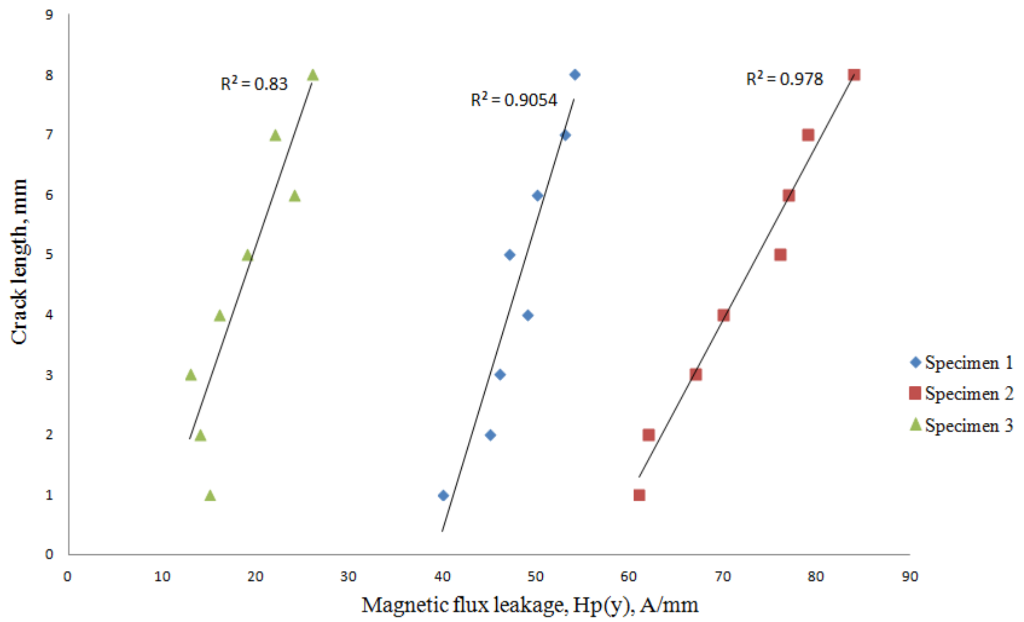

Fig. 12 Linear relation between the crack length and magnetic flux leakage from the MMM signals

which led to the formation of opposite magnetic charges on the crack surface (Dong *et al*. 2012). A longer crack length led to a greater accumulation of magnetic charges, and enhanced the leakage of magnetic flux in the metal's surface and resulted in crack growth. Thus, the axial stress was released and the stress energy was transformed, leading to the generation of a strong magnetic energy. At this time, the crack penetrated through the metal surface and the length of the crack clearly became longer. Moreover, the highest peak value of the magnetic signals for all specimens are stated at 8 mm of crack length with promoting the limit values of 26-84 A/mm. During a cyclic loadings, the bonding of metal structure starts to vibrate and generate a high stress field which enhanced the increment value of the magnetic flux leakage field in the metal surface.

Magnetic flux leakage field was caused by the discontinuity of the crack and the abnormality was caused by stress concentration (Li *et al*. 2003, Roskosz and Bieniek 2012, Dong *et al*. 2009, Yu and Zhang 2010). Basically, the stress concentration occurred because of the increasing residual stress on the metal structure during the loaded cycles. This is because when the load of cycle increases, it will initiate the fatigue crack in the specimen and directly increased the axial stress, σ, thus reduces the effectiveness of the specimen cross-section surface. In addition, a linear relation that is shown in Fig. 12 also has been produced an identical result as stated in previous research from Dong *et al*. 2008, even though they used different materials and dimensions. This result indicates that the MMM method is feasible to determine the length of fatigue crack in specific ferromagnetic structures under definite load cycles. Therefore, it is possible to predict the residual life of ferromagnetic components including crack and defect.

5. Conclusions

From the investigation of magnetic signals induced by tensile loads in mild steel, it can be concluded that a fracture will occur in the zones of stress concentration and can be identified in the event of drastically magnetic flux intensity increase in specimens. The correlation of MMM signals with crack growth rate was identified with the produced curve appearing as a sigmoid shape by replacing the position of ΔK with $Hp(y)$ in the equation of fatigue crack growth. The three regions of crack behaviour of the metal were also analysed in this study. Meanwhile, the linear relation was plotted between the MMM signals with the crack length of the specimens (details about the characteristics of these relations were explained in the previous section). In order to develop the knowledge of MMM, it is suggested that for future studies, other parameters should be taken into account, such as the environmental effect towards MMM signals and the correlation between the MMM signals and stress/strain signals in fatigue analysis.

Acknowledgments

The authors would like to express their gratitude to Universiti Kebangsaan Malaysia and Ministry of Education Malaysia through the fund of FRGS/1/2012/TK01/UKM/01/1 and FRGS/1/2012/TK01/UKM/03/2 for supporting this research project.

References

Annual Book of ASTM Standards (2004), International and Materials, American Society for Testing & Materials.

Beden, S.M., Abdullah, S. and Ariffin, A.K. (2009), “Review of fatigue crack propagation models for metallic components”, *Eur. J. Sci. Res.*, **28**(3), 364-397.

C33 (2004), Standard Specification for Concrete Aggregates, ASTM International West Conshohocken, PA, USA.

Dong, L., Xu, B., Dong, S., Chen, Q. and Wang, D. (2008), “Monitoring fatigue crack propagation of ferromagnetic materials with spontaneous abnormal magnetic signals”, *Int. J. Fatigue*, **30**, 1599-1605.

Dong, L., Xu, B., Dong, S., Song, L., Chen, Q. and Wang, D. (2009), “Stress dependence of the spontaneous stray field signals of ferromagnetic steel”, *NDT&E Int.*, **42**, 323-327.

Dong, L., Xu, B., Dong, S. and Chen, Q. (2010a), “Characterisation of stress concentration of ferromagnetic materials by metal magnetic memory testing”, *Non-destruct. Test. Eval.*, **25**(2), 145-151.

Dong, S., Wang, D., Xu, B. and Shi, C. (2010b), “Characterizing stress concentration by metal magnetic memory signal of H_p (x)”, *Int. J. Appl. Electromagnet. Mech.*, **33**(3-4), 1219-1223.

Dong, L.-H., Xu, B.-S., Wang, H.-P. and Xue, N. (2012), “A physical model for self-emitting magnetic signals during fatigue crack propagation”, *Appl. Mech. Mater.*, **190-191**, 415-418.

Dubov, A.A (1997), “A study of metal properties using the method of magnetic memory”, *Metal Sci. Heat Treat.*, **39**(9), 401-408.

Dubov, A.A., DubovAl, A. and Kolokolnikov, S.M. (2006), “Method of Metal Magnetic Memory (MMM) and inspection instrument”, *International Institute of Welding*.

Dowling, N.E. (1993), *Mechanical Behaviour of Materials: Engineering Methods for Deformation, Fracture, and Fatigue*, Prentice-Hall International Editions.

Huang, H., Jiang, S., Yang, C. and Liu, Z. (2014), “Stress concentration impact on the magnetic memory signal of ferromagnetic structural steel”, *Non-destruct. Test. Eval.*, **29**(4), 377-390.

Li, L., Huang, S., Wang, X., Shi, K. and Wu, S. (2003), “Magnetic field abnormality caused by welding residual stress”, *J. Magnet. Magnet. Mater.*, **261**(3), 385-391.

Milne, I., Ritchie, R.O. and Karihaloo, B.L. (2003), Storage Tank Failures, Comprehensive Structural Integrity Book.

Roskosz, M. and Bieniek, M. (2012), “Evaluation of residual stress in ferromagnetic steels based on residual magnetic field measurements”, *NDT&E Int.*, **45**(1), 55-62.

Wang, Z.D., Yao, K., Deng, B. and Ding, K.Q. (2010a), “Quantitative study of metal magnetic memory signal versus local stress concentration”, *NDT&E Int.*, **43**(6), 513-518.

Wang, Z.D., Yao, K., Deng, B. and Ding, K.Q. (2010b), “Theoretical studies of metal magnetic memory technique on magnetic flux leakage signals”, *NDT&E Int.*, **43**(4), 354-359.

Wang, Z.D., Gu, Y. and Wang, Y.S. (2012), “A review of three magnetic NDT technologies”, *J. Magnet. Magnet. Mater.*, **324**(4), 382-388.

Wu, D., Xu, M. and Li, J. (2010), “Study on physical mechanism of metal magnetic memory technique”, *Appl. Mech. Mater.*, **34-35**, 841-844.

Xing, H., Xu, M., Wang, R. and Zhang, J. (2006), “MMM Fatigue damage evaluation and life prediction modelling for ferromagnetic materials”, *Key Eng. Mater.*, **324-325**, 619-622.

Xing, H., Wang, R., Xu, M. and Zhang, J. (2007), “Correlation between crack growth rate and magnetic memory signal of X45 steel”, *Key Eng. Mater.*, **353-358**, 2293-2296.

Xu, M.X., Xu, M.Q., Li, J.W. and Xing, H.Y. (2012), “Using modified J-A model in MMM detection at elastic stress stage”, *Non-destruct. Test. Eval.*, **27**(2), 121-138.

Yang, L.J., Liu, B., Chen, L.J. and Gao, S.W. (2013), “The quantitative interpretation by measurement using the magnetic memory method (MMM)-based on density functional theory”, *NDT&E Int.*, **55**, 15-20.

Yu, F. and Zhang, J. (2010), “Stress concentration positions determination of ferromagnetic material based on the magnetic test method”, *Key Eng. Mater.*, **417-418,** 865-868.

Zhang, Y.L., Gou, R.B., Li, J.M., Shen, G.T. and Zeng, Y.J. (2012), “Characteristics of metal magnetic memory signals of different steels in high cycle fatigue tests”, *Fatigue Fract. Eng. Mater. Struct.*, **35**(7), 595-605.

CC